J Mater Sci: Mater Med (2016) 27:59
DOI 10.1007/s10856-016-5668-7

BIOMATERIALS SYNTHESIS AND CHARACTERIZATION

Original Research

Exposure of the murine RAW 264.7 macrophage cell line to dicalcium silicate coating: assessment of cytotoxicity and pro-inflammatory effects

Liangjiao Chen[1] · Yanli Zhang[2] · Jia Liu[2] · Limin Wei[2] · Bin Song[2] · Longquan Shao[2]

Received: 15 September 2015 / Accepted: 8 January 2016 / Published online: 22 January 2016

Abstract Inflammatory effects are significant elements of the immune response to biomaterials. Previously, we reported inflammatory effects in response to dicalcium silicate (Ca_2SiO_4, C_2S) particles. However, the immunological effects of C_2S coatings have not been studied. C_2S often used as coatings materials in orthopedic and dentistry applications. It may have different effect from C_2S particles. Further, it remains unclear whether C_2S coating is equally biocompatible as 45S5 coating. The aim of this study was to test the cytotoxicity and pro-inflammatory effects of C_2S coating on RAW 264.7 macrophages. C_2S and 45S5 coatings were characterized using scanning electron microscopy (SEM), atomic force microscopy (AFM), energy dispersive analysis (EDS) and X-ray diffraction (XRD). inductively coupled plasma optical emission spectroscopy (ICP-OES) was used to detect ionic concentrations after soaking coated discs in medium. The cytotoxicity of C_2S and 45S5 coatings against RAW 264.7 macrophages was measured using the LDH Cytotoxicity Assay Kit, Cell Counting Kit-8 (CCK-8) assays and flow cytometry for apoptosis assays. The gene and protein expression of TNF-α, IL-6 and IL-1β were detected using RT-q PCR and ELISA, respectively. The tested coating materials are not cytotoxic to macrophages. The C_2S-coated surface stimulated macrophages to express pro-inflammatory mediators, such as TNF-α, IL-6 and IL-1β, and C_2S coating caused less IL-6 but greater IL-1β production than the 45S5 coating. C_2S coating have no cytotoxicity when directly cultured with macrophages. C_2S and 45S5 coatings both have the potential to induce pro-inflammatory effects, and the biocompatibility of C_2S is similar to that of 45S5.

1 Introduction

$CaO–SiO_2$-based materials are often used as coating materials or bone substitute scaffolds [1]. Dicalcium silicate (Ca_2SiO_4, C_2S) is a new bioactive inorganic material that consists of silicon, calcium and oxygen, which composed of $CaO–SiO_2$ component [2]. Silicon ions released from C_2S coating play an important roles in skeletal development and repair [3]. Plasma-sprayed C_2S coating exhibits better bioactivity and bonding strength to titanium substrates than plasma-sprayed HA coatings [4]. When C_2S, either alone or in combination with titanium particles or poly (D, L-lactic acid) (PDLLA), was immersed in simulated body fluid (SBF) for several days, the formation of bone-like HA was induced, which indicated good bioactivity and long-term durability [5]. Favorable biological properties were demonstrated by studying the adhesion and differentiation of human osteogenic cells that were seeded directly on a dicalcium silicate-coated surface [6]. In dentistry, C_2S cement can be used as a root-end filling and a pulp-capping material [7] and is significantly less cytotoxic than the traditional root-end filler, mineral trioxide aggregate (MTA) [8]. C_2S cement is also a model for drug release [9], and C_2S possesses excellent bioactivity when used as a coating

Liangjiao Chen and Yanli Zhang have contributed equally to this work and should be considered co-first authors.

✉ Longquan Shao
shaolongquan@smu.edu.cn

[1] Key Laboratory of Oral Medicine, Guangzhou Institute of Oral Disease, Stomatology Hospital of Guangzhou Medical University, Guangzhou 510140, People's Republic of China

[2] Department of Stomatology, Nanfang Hospital, Southern Medical University, 1838 North Guangzhou Road, Guangzhou 510515, People's Republic of China

material for titanium alloy substrates [10]. These findings support the future broad use of C_2S in orthopedic and dentistry applications.

Ideal implant coating materials should induce good osteogenic effects and limited pro-inflammatory effects to produce biocompatible coated implants that exhibit a long postoperative life span [1]. The pro-inflammatory effect is a significant element of the host response to implanted biomaterials, as such, this effect is one of the key indicators to evaluate biocompatibility. This effect causes the risk of aseptic inflammation, which may result in implant loosening. Based on multiple retrieval studies, macrophages can play significant roles in determining the duration and intensity of the inflammatory response and in the mechanism behind implant failure [11–13]. Many coating materials and bone substitute materials can activate macrophages at the bone-implant interface, possibly leading to bone resorption and implant failure [14, 15]. Generally, hydroxyapatite ($Ca_{10}(PO_4)_6(OH)_2$, HA) is considered a relatively safe coating material due to its bioactivity and biocompatibility [16]. However, particle release from the prosthesis can cause aseptic inflammation. For example, the interaction between HA particles and human monocytes causes the production of inflammatory mediators, including tumor necrosis factor alpha (TNF-α) and IL-6 [17–19]. In a previous study, we suggested that C_2S particles also cause pro-inflammatory effects [20]. However, C_2S is often used as a coating material. The immunological effects of C_2S coating, which releases ions when in contact with monocytes/macrophages, have not been studied in detail. Therefore, it is necessary to evaluate the potential pro-inflammatory effects of C_2S coating before widespread clinical use.

Bioglass 45S5, a traditionally used bioactive glass that contains 45 % silicon dioxide, has been shown to stimulate osteogenesis in vitro and in vivo [21]. 45S5 is an ideal candidate material due to its osteostimulative properties. However, this material has not been formulated in a manner that exhibits stability to devitrification or thermal expansion coefficients (TECs) that are suitable for stable coating onto metal implants while retaining its bioactive properties [22]. Previous studies indicate that the topical application of 45S5 bioactive glass in humans with experimental gingivitis attenuated the clinical signs of inflammation; however, bacterial accumulation was not inhibited [23]. 45S5 glass significantly reduced the amount of TNF-α and IL-6 secreted by LPS- stimulated macrophages and monocytes as compared to cells that were stimulated in the absence of bioactive glass [24]. Other studies have indicated that 45S5 bioglass powders increase the release of TNF-α by peritoneal macrophages and monocytes [25]. Controversy surrounds the pro-inflammatory effect of 45S5 powders, and the potential pro-inflammatory effects of 45S5 coating have not been studied. It remains to be determined whether C_2S coating is equally biocompatible as 45S5 coating.

Therefore, we aimed to investigate the cytotoxicity of this biomaterial coating, to examine whether C_2S and 45S5 coatings induce the release of pro-inflammatory mediators in mouse macrophages, and to determine which material is more biocompatible.

2 Materials and methods

2.1 Preparation of dicalcium silicate and 45S5 coatings

C_2S powder with typical particle sizes of 5-30 μm and 45S5 powder with typical particle sizes of 18–100 μm were synthesized in the laboratory of the Shanghai Institute of Ceramics at the Chinese Academy of Sciences. An atmosphere plasma spray (APS) system (Sulzer Metco, Switzerland) was applied to fabricate the coating on a Ti–6Al–4 V substrate (Northwest Nonferrous Metal Academy, Xian, China) with dimensions of 10 mm × 10 mm × 1 mm, as previously reported [26]. All substrates were sandblasted. The spray parameters were as follows: argon (40 slpm) and hydrogen (12 slpm) were used as primary and auxiliary plasma-forming gases, respectively. The powder feeding rate was approximately 20 g/min using argon (3 slpm) as a carrying gas. The plasma arc current and voltage were 600 A and 73 V, respectively. The spraying distance was 90 mm.

2.2 Characterization of C_2S and 45S5 coatings

Surface morphologies were observed by scanning electron microscopy (SEM; Nova Nano SEM 430, FEI, Finland) and atomic force microscopy (AFM; Asylum Research, USA) Elemental analysis were determined by energy-dispersive X-ray spectroscopy (EDS; DX-4 system, EDAX, USA). Crystal structures were analyzed using X-ray diffraction (XRD; Geigerflex, Rigaku Co, Japan); the diffraction pattern was measured in the 2θ range from 10° to 80° using monochromatic Cu Kα radiation.

After ultrasonic washing in acetone and rinsing in deionized water, five pieces of C_2S and 45S5 coating plates were soaked in 100 mL Dulbecco's Modified Eagle's Medium (DMEM; Gibco, USA) at 37 °C for 72 h under static conditions. The concentrations of released calcium (Ca), silicon (Si), and phosphorus (P) ions in the medium were measured using inductively coupled plasma optical emission spectroscopy (ICP-OES). The ionic concentrations of these ions in normal DMEM were measured as a control.

2.3 Estimation of endotoxin levels on dicalcium silicate and 45S5 coatings

The coated samples were ultrasonically washed in acetone and rinsed in deionized water and then disinfected using autoclaving. The sterilized temperature is 121 °C and pressure is 103.4 kPa for 15 min. Coating and packaging procedures were subject to continuous endotoxin control. Particle endotoxin levels were measured using an E-Toxate Kit (Sigma, St. Louis, USA) to exclude the possibility of proinflammatory effects arising from bacterial contamination of the coated discs. The discs were dropped into endotoxin-free water and incubated with *Limulus polyphemus* in sterilized glass tubes at 37 °C, and gel formation was evaluated after 1 h.

2.4 Cell culture

The mouse macrophage cell line RAW 264.7 (American Type Culture Collection, TIB71, MD, USA) was used to evaluate cytotoxicity and cytokine production induced by the C_2S and 45S5 discs. Cells were maintained in DMEM supplemented with 10 % fetal calf serum (Life Technologies, USA), glutamine (2 mM), penicillin (5000 U mL^{-1}) and streptomycin (25 μg mL^{-1}) at 37 °C under a saturated 5 % CO_2, 95 % air atmosphere. Cells were exposed to coated or uncoated Ti–6Al–4 V discs. Negative controls without discs were also examined. Culture medium containing 0.64 % phenol solution was used as a positive control to evaluate cell viability. Cells cultured in DMEM with 10 μg/mL lipopolysaccharide (LPS, Sigma St. Louis, USA) were used as positive controls to evaluate cytokine production.

2.5 Cell cytotoxicity and apoptosis profiles in response to dicalcium silicate and 45S5-coated disc exposure

C_2S- and 45S5-coated discs (3 pieces) were placed on 24-well plates; RAW 264.7 macrophages were then seeded into the wells at a total density of 2×10^5 cells and incubated for 24 h and 48 h. The control group and Ti–6Al–4 V substrate without coated discs were also incubated. In the positive control group, macrophages were incubated in plates without coated discs but with medium containing 0.64 % phenol solution. Cell cytotoxicity was observed using the LDH Cytotoxicity Assay Kit, and cell proliferation response was evaluated using the Cell Counting Kit-8 assay (CCK-8, Dojindo, Japan). The results were confirmed by flow cytometry using a FITC Annexin V Apoptosis Detection Kit (Dojindo, Japan) according to the manufacturer's instructions. Briefly, cells were stained with FITC-conjugated annexin V (FITC-V) and propidium iodide (PI). Viable, early apoptotic and late apoptotic and/or necrotic cells were identified as annexin V−PI−, annexin V+PI− and annexin V+PI+, respectively. Data were acquired using a FACSCalibur (BD Biosciences, San Jose, USA) flow cytometer and Cell Quest software (BD Biosciences), and the results were analyzed using Flow Jo software.

2.6 Real time quantitative reverse transcription polymerase chain reaction (q RT-PCR) analyses of steady-state mRNA levels of pro-inflammatory mediators

RAW 264.7 cells were cultured in 6-well plates in the presence of five pieces of coated or uncoated discs for 6 h and 24 h. After 6 h and 24 h, RT-qPCR was used to detect the expression of TNF-α, IL-6, and IL-1β. Total RNA was extracted using RNAiso Plus (Takara, Japan). RNA (1 μg) obtained from each sample was reverse-transcribed using oligo-dT as the first-strand cDNA primer (Revert Aid First Strand cDNA Synthesis Kit, Thermo Scientific, USA). Primer sequences and the length of fragments for TNF-α, IL-6, and IL-1β and GAPDH are described in Table 1. Reverse transcribed cDNA was subjected to q-PCR (SYBY Premix Ex Taq, Takara, Japan) using the following cycling conditions: 95 °C for 10 min (initial denaturation), followed by 40 cycles of 95 °C for 15 s and 60 °C for 60 s, and then 60 °C for 5 min for terminal extension; from 75 to 95 °C, the temperature was elevated one degree each 20 s to obtain a melting curve. The $\Delta\Delta C_T$ method of relative quantification was used to determine the fold change in expression. Delta Ct (ΔCT) represents the difference between the target Ct value and the control Ct value for each sample: $\Delta C_T = Ct_{target} - Ct_{control}$. The expression was further normalized using the control ($\Delta\Delta CT = \Delta C_T - CT_{control}$). The fold change in expression was then obtained as 2ΔΔCT, and a graph was plotted of log 2ΔΔCT.

2.7 Cytokine production measured using ELISA

After 6 and 24 h of incubation, the supernatants were collected and centrifuged at 1000 g for 15 min. TNF-α,

Table 1 Primers used for real-time PCR

Name	Primer
TNF-α	AACTCCAGGCGGTGCCTATG
	TCCTCCACTTGGTGGTTTGTG
IL-6	GAAATGATGGATGCTACCAAACTG
	GACTCTGGCTTTGTCTTTCTTGTT
IL-1β	TCAAATCTCGCAGCAGCACATC
	CGTCACACACCAGCAGGTTATC
GAPDH	AGGAGCGAGACCCCACTAACA
	AGGGGGGCTAAGCAGTTGGT

IL-6, and IL-1β were measured using a commercial ELISA kit (Biolegend, San Diego, USA). The sensitivities of the ELISA kit were 4 pg/mL for TNF-α, 2.0 pg/mL for IL-6 and 16.0 pg/mL for IL-1β.

2.8 Statistical analysis

Bar graphs were used to show the mean and standard deviation (SD) of triplicate experiments. The data were normalized, and data that passed the normality test were analyzed using one-way ANOVA with the least significant difference (LSD) test and Dunnett's test for abnormal distribution. All analyses were conducted using SPSS 17.0 software (SPSS Inc., Chicago, IL, USA). *P* values <0.05 were considered significant.

3 Results

3.1 Characterization of dicalcium silicate and 45S5 coatings

The surface morphology of the coatings was evaluated using SEM and AFM. After sandblasting, the substrate surface was rough (Fig. 1a). The C_2S- and 45S5 coatings exhibited different surface topographies according to SEM, (Fig. 1b, c). Three-dimensional AFM images (Fig. 2) displayed the surface topography of the sandblasting substrates, C_2S- and 45S5-coated discs. Roughly surfaces were observed on the surface of the sandblasting disc (200.15 ± 40.47 nm) (Fig. 2a). After coating, the obviously roughness were appeared on the C_2S coating and 45S5 coating (C_2S 633.16 ± 43.14 nm, 45S5 461.23 ± 38.24 nm) (Fig. 2b, c). The roughness of the C_2S coating and 45S5 coating were significantly greater than that of the sandblasting disc (Fig. 2d). Because of the different materials loaded onto the substrates, the roughness of C_2S coating was significantly greater than 45S5 coating (Fig. 2d).

EDS analysis showed that Ca, Si, and O were present on the surface of the dicalcium silicate coating and that Ca, Si, P, and O were present on the surface of the bioglass 45S5 coating (Fig. 1e, f). In the XRD analysis, the phase pattern seen in Fig. 3a corresponds to dicalcium silicate [10], and the phase pattern seen in Fig. 3b corresponds to bioglass 45S5 [27]. The peaks have been labeled in the figures.

The ionic concentrations of Si, Ca, and P in the C_2S/45S5 coating medium and normal DMEM analyzed by ICP-OES are illustrated in Table 2. The results showed a significant increase in Si concentration in the DMEM media after allowing C_2S and 45S5 coatings to soak in these media for 72 h at 37 °C. The Si concentration of the C_2S coating

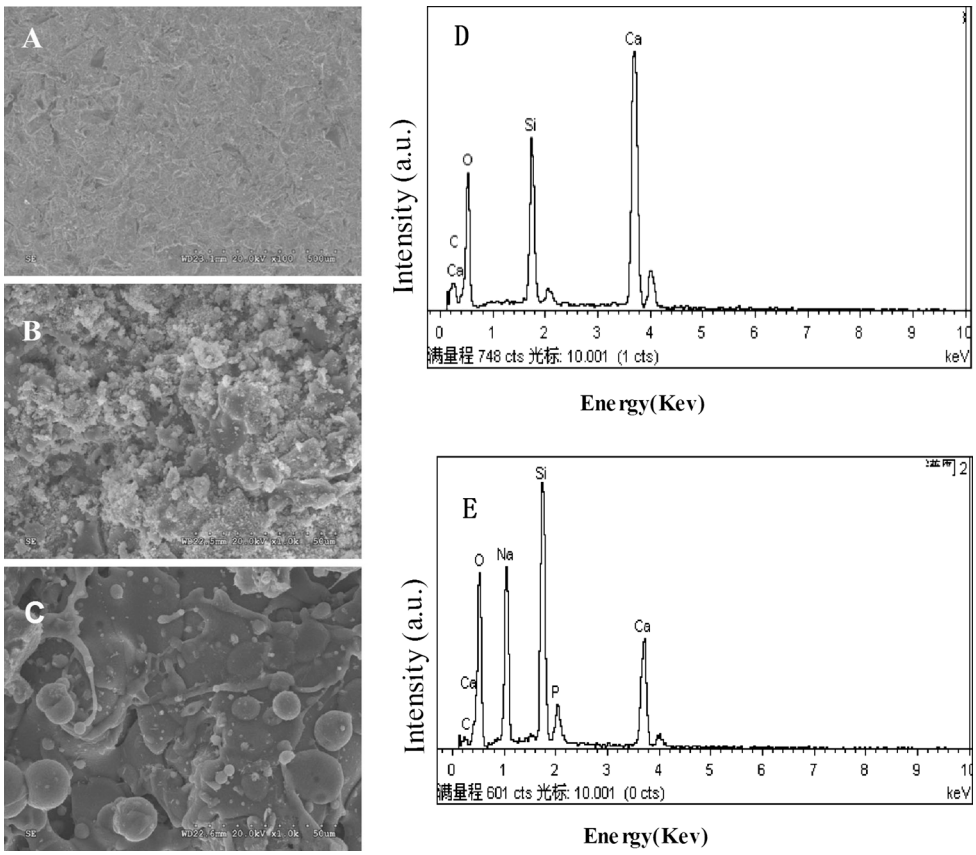

Fig. 1 SEM photographs and EDS analysis of the sprayed coating surfaces. SEM shows the surface topography of the sandblasted titanium plate and the two coatings (1,000X), whereas EDS analysis shows the elemental composition of the C_2S and bioglass 45S5 coating surfaces. SEM: **a** sandblasted titanium plate; **b** C_2S coating surface; **c** 45S5 coating surface. EDS: **d** C_2S; **e** 45S5

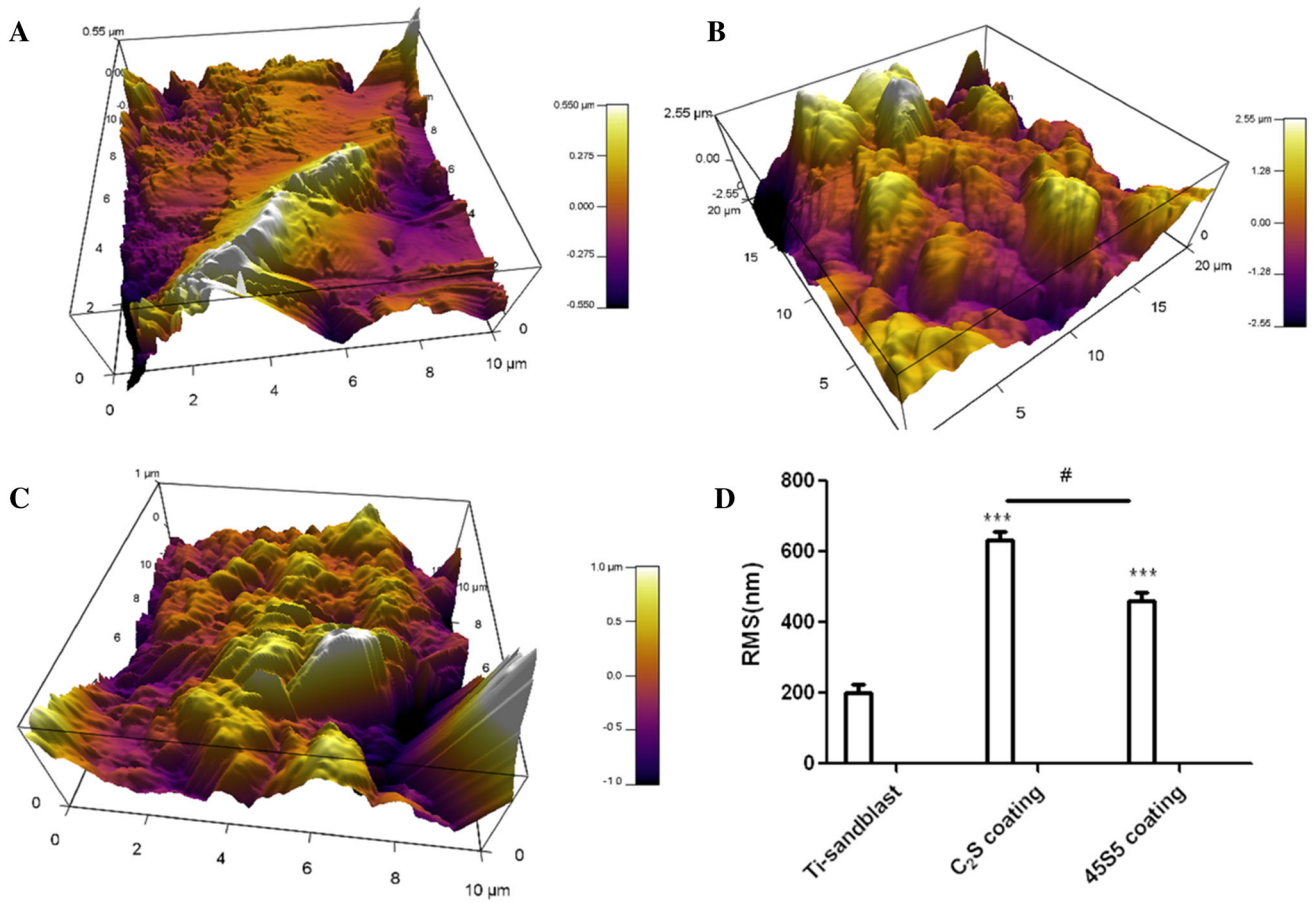

Fig. 2 Surface morphology analysis of different surfaces using AFM and a comparison of roughness. **a** sandblasting substrate, **b** C_2S coating surface, **c** 45S5 coating and **d** the surface roughness of the specimens. The roughness of the C_2S and 45S5 were significantly greater than that of the sandblasting substrate. The roughness of C_2S coating was significantly greater than 45S5 coating (*** $P < 0.01$ when compared to the sandblasting substrate. # $P < 0.05$ when compared to the C_2S coating group)

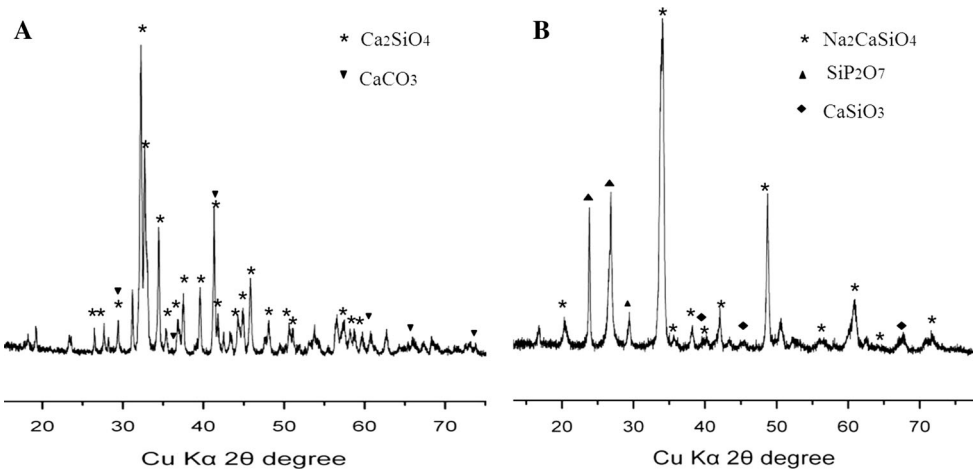

Fig. 3 XRD pattern of the sprayed coatings. **a** Dicalcium silicate coating; **b** bioglass 45S5 coating The peaks have been labled

medium was nearly 29 times that in DMEM ($P < 0.05$) and nearly 20 times of the 45S5 coating medium. The Si concentration was higher in the 45S5 coating medium than in the C_2S coating medium, and the difference between the groups was significant ($P < 0.05$). The concentrations of P and Ca in the C_2S coating medium were slightly lower than those in DMEM. However, the P and Ca concentrations in the 45S5 coating medium were slightly higher.

Table 2 Ion concentrations in coating media (Mm) (x ± s n = 3)

	DMEM	C_2S medium	45S5 medium
Si	0.003 ± 0.00	0.087 ± 0.017*	0.064 ± 0.016*#
Ca	1.730 ± 0.216	1.512 ± 0.171	2.012 ± 0.230
P	1.052 ± 0.311	1.024 ± 0.149	1.152 ± 0.144

* P 0.05 when compared to the control group

P 0.05 when compared to the C_2S coating group

3.2 The cytotoxicity profiles of the dicalcium silicate and 45S5 coatings

Cellular cytotoxicity was evaluated using an LDH Cytotoxicity Assay Kit (Biyuntian, China) according to the manufacturer's instructions. No obvious cytotoxicity was detected after RAW 264.7 macrophages were cultured with C_2S- and 45S5-coated discs after 24 h and 48 h (Fig. 4a), and more than 50 % cell death was observed in the positive control group. Approximately 4-6 % cell mortality was observed for the control group, and mortality rates of approximately 5–7 and 7–8 % were found in the C_2S and 45S5 groups, respectively. Cell proliferation was evaluated using CCK-8 assays. In the coated disc groups, more than 90 % of the cells were viable, and approximately 40 % of cells remained viable in the positive control group (Fig. 4b).

Cells were stained with FITC-conjugated annexin V and PI in apoptosis analysis. Viable, early apoptotic and late apoptotic and/or necrotic cells were identified as annexin V−PI−, annexin V+PI− and annexin V+PI+, respectively. Figure 5 showed that no obvious difference of apoptosis was detected after culturing RAW 264.7 macrophages with the C_2S/45S5-coated discs when compared with control group. There was no difference between C_2S and 45S5 group. Approximately more than 50 % apoptosis was observed in the positive control group (Fig. 5).

3.3 mRNA and protein expression of TNF-α, IL-6 and IL-1β

To determine the effects of the discs on proinflammatory mediator expression in macrophages, steady-state mRNA levels of TNF-α, IL-6 and IL-1β were determined using RT-q PCR and ELISA. The cells were harvested after cultivation for 6 or 24 h. LPS-treated cells were used as positive controls. Constitutive low levels of TNF-α mRNA were observed for the uncoated, C_2S-coated and 45S5-coated plates after 6 h ($P > 0.05$). At this time, high levels of TNF-α mRNA were observed in the positive controls ($P < 0.05$, Fig. 6a). After 24 h, TNF-α mRNA expression was significantly increased in the 45S5 coating group ($P < 0.05$, Fig. 6a); however, the C_2S coating group had a weaker effect on TNF-α mRNA expression than the control group ($P > 0.05$, Fig. 6a). No significant difference in TNF-α mRNA expression was observed between the C_2S and 45S5 coatings ($P > 0.05$).

Next, we examined IL-6 mRNA levels. No significant increase in IL-6 mRNA was detected after 6 h of cultivation with either the uncoated plates or the C_2S-coated plates (Fig. 6b). A significant increase of IL-6 mRNA was observed for the 45S5 group. A significant difference was also observed between the C_2S and 45S5 groups. The positive control group expressed high levels of IL-6 mRNA after 6 and 24 h of cultivation ($P < 0.05$). After 24 h, the expression of IL-6 mRNA was not significantly altered in the uncoated, C_2S and 45S5 groups ($P < 0.05$).

Subsequently, IL-1β mRNA expression was detected (Fig. 6c). LPS induced high levels of IL-1β expression after 6 and 24 h. C_2S caused a slight increase in IL-1β expression after 6 h. However, no differences were noted in the C_2S and 45S5 groups after 6 h and 24 h ($P > 0.05$) (Fig. 6c). After 24 h, C_2S and 45S5 significantly promoted IL-1β mRNA expression ($P < 0.05$).

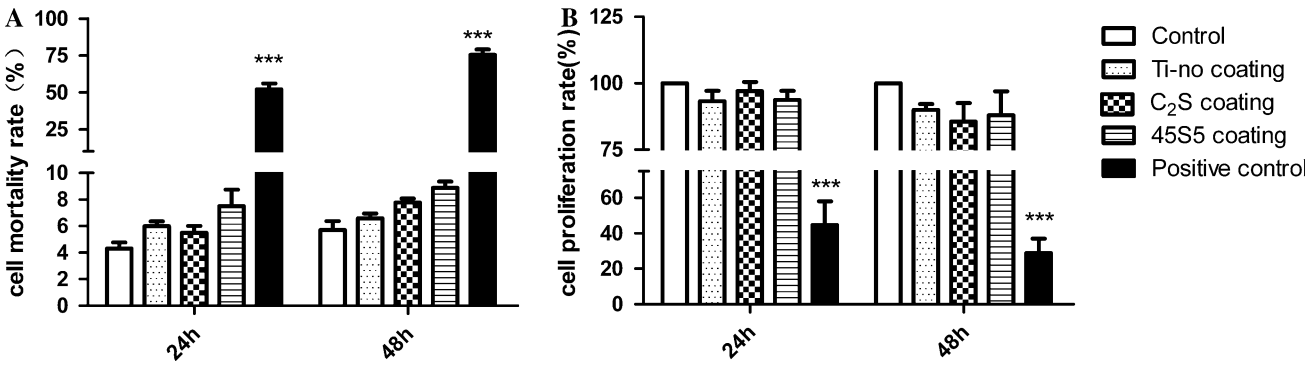

Fig. 4 Cell cytotoxicity (**a**) and proliferation (**b**) of RAW264.7 cells exposed to C_2S- and 45S5-coated surfaces for 24 and 48 h. **a** No obvious cytotoxicity was detected after RAW 264.7 macrophages were cultured with C_2S- and 45S5-coated discs, and more than 50 % cell death was observed in the positive control group. Approximately 4–6 % cell mortality was observed for the control group, and mortality rates of approximately 5–7 and 7–8 % were found in the C_2S and 45S5 groups, respectively. **b** More than 90 % of the cells were viable, and approximately 40 % of cells remained viable in the positive control group

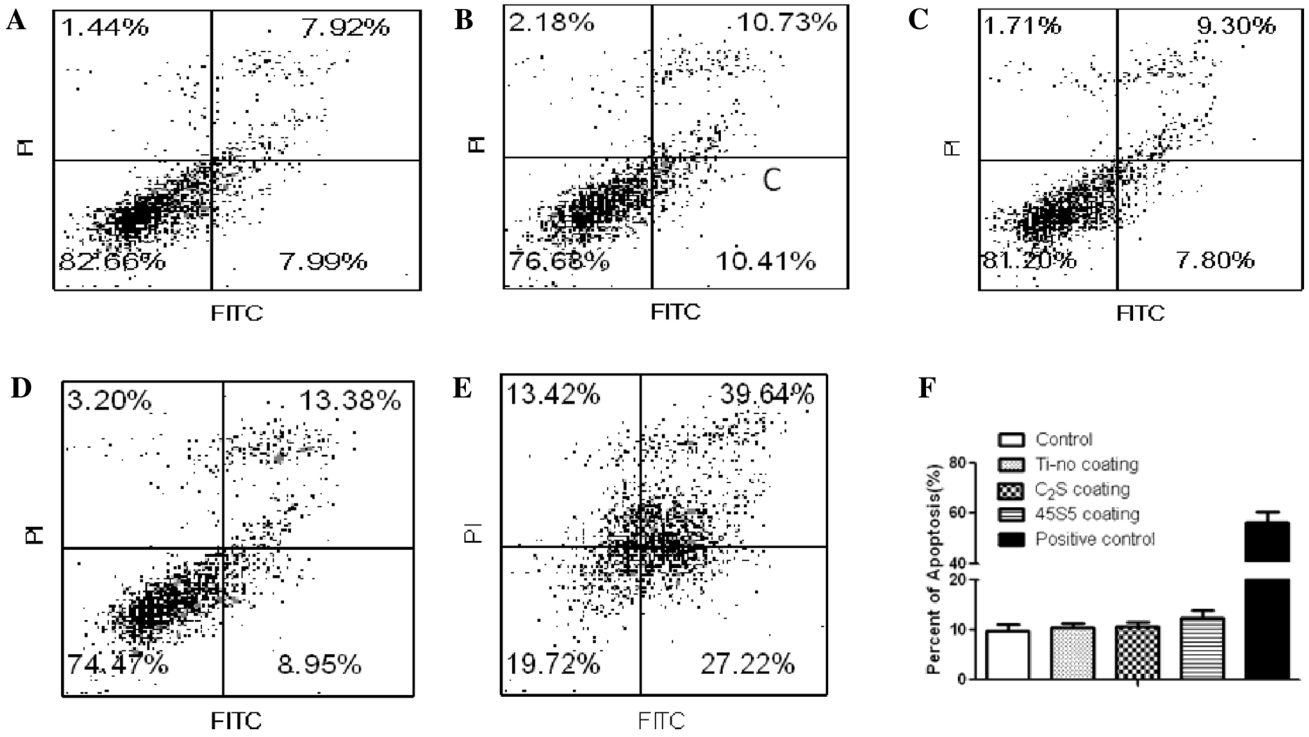

Fig. 5 No obvious signs of apoptosis were observed when cells were stained with FITC-conjugated annexin V and PI. Viable, early apoptotic and late apoptotic and/or necrotic cells were identified as annexin V−PI−, annexin V+PI− and annexin V+PI+, respectively. Graphical representations of normally cultured RAW264.7 cells (**a**) and RAW264.7 cells cultured with uncoated plates, C_2S-coated Ti plates, 45S5-coated Ti plates (**b**, **c**, and **d**, respectively) and 0.64 % phenol solution (**e**). Approximately 9 % of RAW264.7 cells underwent apoptosis in the control group, and approximately 10 % of the cells underwent apoptosis in the uncoated, C_2S-coating and 45S5-coating groups. No significant difference was found among these groups (**f**). All values are represented as the mean ± SD of triplicate experiments

3.4 Pro-inflammatory cytokine production

Based on our RT-qPCR results, ELISAs were used to detect the effects of C_2S and 45S5 on the production of TNF-α, IL-6 and IL-1β after 24 h. TNF-α concentrations were increased in the C_2S and 45S5 groups compared to the control group ($P < 0.05$). No significant differences in TNF-α concentration were observed between the C_2S and 45S5 groups (control: 5.61 ± 2.96 pg/mL, uncoated group: 33.33 ± 0.59 pg/mL, C_2S: 43.90 ± 3.66 pg/mL, 45S5: 44.84 ± 2.25 pg/mL, positive control group: 609.72 ± 208.48 pg/mL, Fig. 6d). Nevertheless, C_2S and 45S5 induced a larger increase in TNF-α concentration than the uncoated Ti group ($P < 0.05$).

Next, we examined IL-6 levels (Fig. 6e). IL-6 concentration was greatly altered in the uncoated and C_2S and 45S5 coating groups. 45S5 triggered a stronger increase in IL-6 expression than C_2S ($P < 0.05$) (control: 4.08 ± 2.34 pg/mL, uncoated Ti: 13.54 ± 2.84 pg/mL, C_2S:16.15 ± 4.69 pg/mL, 45S5: 22.82 ± 2.04 pg/mL, positive control: 98.16 ± 26.75 pg/mL Fig. 5e).

Finally, we measured the IL-1β concentration in all groups. C_2S induced a greater than two-fold increase in IL-1β production when compared with 45S5, more than three-fold increase with non-coating group and more than four-fold increase with contro group (control: 2.99 ± 2.40 pg/mL, uncoated Ti: 5.07 ± 1.68 pg/mL, C_2S:18.37 ± 0.50 pg/mL, 45S5: 7.43 ± 5.19 pg/mL, positive control: 90.38 ± 13.25 pg/mL Fig. 6f). LPS strongly induced IL-1β expression.

To our knowledge, this study is the first to examine the effect of a C_2S-coated surface on TNF-α, IL-6 and IL-1β production. C_2S coating caused less IL-6 production but greater IL-1β production than 45S5 coating.

4 Discussion

Although many studies have indicated that C_2S coatings exhibit favorable bioactivity and bioconductivity [28, 29], the biocompatibility of this coating, its interaction with immune cells, and the potential pro-inflammatory effects of C_2S have not been previously explored. Due to their different material morphology and reaction with different immune cell lines, C_2S coating might exhibit different cellular responses and pro-inflammatory effects than C_2S particles. When determining the potential risks of C_2S as an coating material, the study of coatings is more relevant than

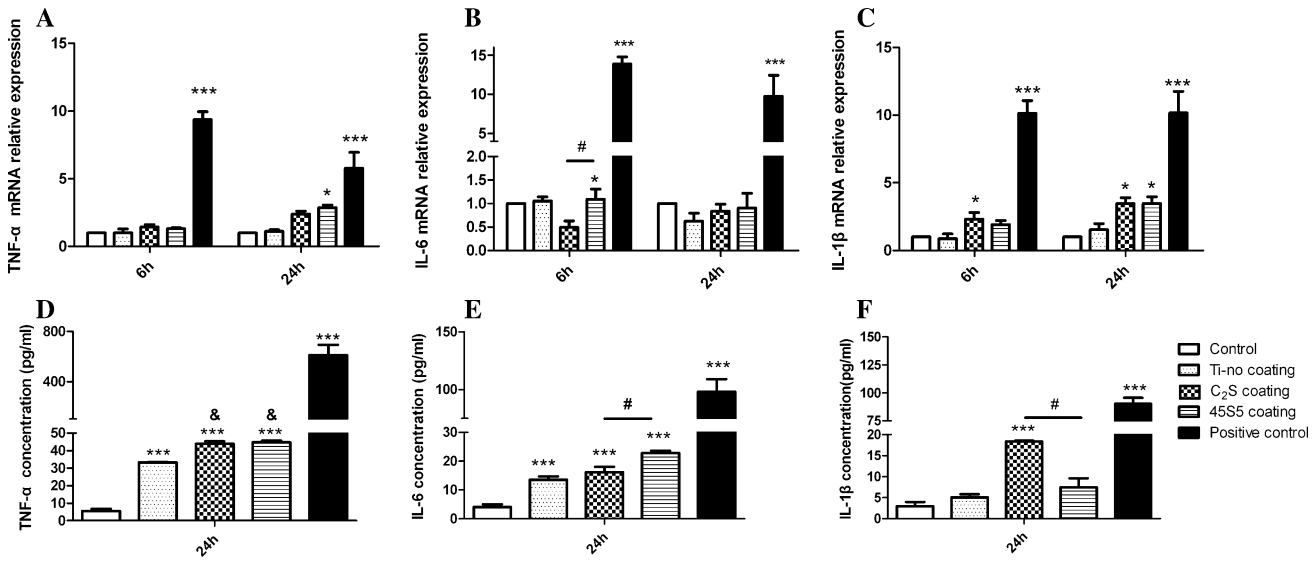

Fig. 6 mRNA and protein expression of pro-inflammatory mediators. A, B and C represent TNF-α, IL-6 and IL-1β mRNA expression, respectively. 45S5 coating increased the expression of TNF-α after 24 h and increased the expression of IL-6 after 6 h. 45S5 coating increased the expression of IL-6 to a greater extent than C_2S coating, and both C_2S and 45S5 coating increased the expression of IL-1β. D, E, and F show the production of TNF-α, IL-6 and IL-1β after 24 h, respectively. 45S5 increased IL-6 to a greater extent than C_2S, but C_2S increased the expression of IL-1β to a greater extent than 45S5. The data are expressed as the mean ± SD. * $P < 0.05$, ** $P < 0.01$ and *** $P < 0.001$ (experimental group vs. control). $^{\#}$ $P < 0.05$, $^{\#\#}P < 0.01$ and $^{\#\#\#}P < 0.001$ (C_2S vs. 45S5). $^{\&}$ $P < 0.05$, $^{\&\&}$ $P < 0.01$ and $^{\&\&\&}$ $P < 0.001$ (experimental group vs. uncoated Ti group)

the study of particles. The aim of this study was to evaluate cytotoxicity and pro-inflammatory mediator production in macrophages in response to C_2S- and 45S5-coated discs. Our results demonstrated that C_2S- and 45S5-coated discs are not toxic to RAW 264.7 macrophages. However, they do exhibit potential pro-inflammatory effects.

C_2S and 45S5 are often considered potential coating materials for prosthetic orthopedic and dental implants [6, 30]. Plasma spraying represents an effective way to prepare C_2S and 45S5 coatings [31, 32]. In this study, we prepared coated discs using the plasma spraying technique. EDS and XRD analyses indicated that the biomaterials were successfully coated onto the substrate. ICP-OES analysis showed that ions were released from the coating substrate after soaking in medium. Ions, such as Si, Ca and P, are dissipated from C_2S and 45S5. Therefore, the C_2S and 45S5 coatings were successfully prepared.

We used the murine cell line RAW 264.7 because of its close resemblance to human macrophages, which are seen in the proximity of prosthesis and cement [33]. To differentiate TNF-α, IL-6 and IL-1β responses at early and late stages, the mRNA expression levels of these cytokines were analyzed at 6 and 24 h post-treatment (at the times selected for the analysis of cell-powder interaction [34]. Based on the obtained mRNA expression data, protein levels were measured after 24 h of treatment [35]; thus, the macrophages interacted with the surfaces over a sufficient period [36].

Previous studies have shown that cytokine production and osteoclast differentiation are stimulated by adherent endotoxins on wear particles [37]. Therefore, our discs were disinfected using autoclave and tested for endotoxins to ensure that the discs were free of contamination. Autoclaving was often used in other dicalcium silicate coating researches [38, 39]. This is a common disinfection method for coating implant in vitro or in vivo studies [40, 41].

Most studies have focused only on the safety and osteogenic effects of the ionic products of C_2S and 45S5 [21, 42]. In our previous study [20], C_2S particles were shown to produce no obvious cytotoxicity in THP-1, PBMC and MG-63 cells. The cytotoxicity of C_2S- and 45S5-coated surfaces has never been evaluated when directly cultured with macrophages. In the present study, RAW 264.7 macrophages were cultured directly with coated surfaces. The results of the LDH cytotoxicity assay indicated that the cell mortality rate was low in both the C_2S and 45S5 groups. CCK-8 assays showed that the C_2S and 45S5 groups did not significantly decrease cell proliferation. In addition, no significant apoptosis was observed. These results confirmed that C_2S was not cytotoxic to macrophages when used as a coating material in vitro.

The general mechanism for the bio-conductivity of CaO-SiO_2-based coatings involves the dissolution of calcium and silicon ions from the coating to increase the calcium concentration between the bone and implant [43, 44]. Higher calcium and silicon concentrations promote the

apatite precipitation on implant surfaces and rapid integration of the implant into existing bone, thereby improving healing time significantly. The ionic dissolution products of C_2S coatings promote human mesenchymal stem cell (hMSC) proliferation and osteogenic differentiation [38] and might up-regulate osteoblast differentiation [39], enhance the expression of osteoblast-related genes, and promote the differentiation of MG-63 cells during an initial period [45]. Ionic dissolution products of Bioglass 45S5 result in enhanced collagen type 1 and osteocalcin expression in human periodontal ligament fibroblasts [46]. In the present study, Si concentrations were significantly increased in DMEM after C_2S- and 45S5-coated surfaces were soaked in this medium. The concentrations of P and Ca decreased in the medium when C_2S-coated discs were used but increased when 45S5-coated discs were used. This result indicates that the ionic dissolution products of C_2S and 45S5 coatings differ and might have different biological effects and potential risks.

Previous studies have indicated that Toll-like receptor 4 (TLR4) plays a vital role in the pro-inflammatory interaction between cells and biomaterials [47]. TLR4 is involved in the uptake of particles, such as titanium dioxide nanoparticles (TiO_2 NPs), to promote inflammatory responses [48]. Furthermore, wear-debris particles from implants use TLR4 signaling to stimulate macrophages [49]. Toll-like receptor activation, such as that caused by TNF-α and IL-6, is involved in the response to implant debris or coating ions that cause progressive pathological bone loss or "aseptic loosening" [50]. Previous studies have demonstrated that surface topography (in particular, that of surfaces that have been subjected to sandblasting and acid etching) modulates the expression of pro-inflammatory cytokines and chemokines by macrophages in a time-dependent manner. These cytokines and chemokines include IL-6 and TNF-α. IL-1β was undetectable in un-stimulated macrophage cultures on all surfaces at all times tested [51]. Similar research also indicates that other surface topographies also cause pro-inflammatory cytokine expression and pro-inflammatory signaling [52, 53]. The data presented here show that sandblasted and uncoated surfaces can induce cytokine production when in direct contact with macrophages. The sandblasting of uncoated surfaces promoted TNF-α and IL-6 production but had no effect on IL-1β production, consistent with previous studies.

Calcium phosphate-coated surfaces stimulate polymorphonuclear neutrophils (PMNs) to significantly release IL1β and TNFα [54]. In addition, HA coatings induce a pro-inflammatory cytokine response in murine J774A.1 macrophages [36]. These results indicate that coated substrate surfaces might provoke aseptic inflammation. In the current study, C_2S-coated surfaces significantly increased the expression and production of TNF-α. The effect of C_2S-coated surfaces on TNF-α is consistent with the results of previous studies on C_2S particles [20]. In addition, C_2S-coated surfaces significantly increased the production of IL-6 and IL-1β, possibly due to the release of ions or particles from the coated surfaces. In previous study, porous titanium modified by silicate calcium can decreased the macrophage adherence and up-regulated the release of several pro-inflammatory mediators, including TNF-α, IL-6, IL-12 [55]. In the present study, 45S5-coated surfaces which also release Si ions induced cytokine production when directly in contact with RAW264.7 cells. These studies indicated that silicate-based materials may also provoke aseptic inflammation. The different concentrations of P and Ca may play an important role in the different pro-inflammatory effect between C_2S and 45S5. The different topography of the coating surface might also make this difference [52, 53]. C_2S caused greater IL-1β production but less IL-6 production than 45S5, possibly due to the different ionic concentrations and surface topographies of the coated discs.

5 Conclusion

In this study, we demonstrated that C_2S coating is not cytotoxic against RAW264.7 macrophages. C_2S coated surface increased the production of TNF-α, IL-6 and IL-1β when compared with non-coating surfaces. Furthermore, C_2S coating had less influence on IL-6 expression but more influence on IL-1β expression than 45S5. These results indicate that, similar to 45S5, C_2S might be a safe biomaterial. Therefore, these findings provide evidence supporting the choice and widespread use of C_2S as a coating for prostheses and dental implants as well as for use with bone substitutes. This work will be extend to primary human macrophages in our further study.

Acknowledgments This work was supported by the National Natural Science Foundation of China (31070857 and 50973045) and the Project on the Integration of Industry, Education and Research of Guangdong Province, China (2012B091000147). This work was also supported by Medical Research Foundation of Guangdong Province (A2015132) and Scientific research projects of Guangzhou Medical University (2015C43).

References

1. Wu C, Chen Z, Yi D, Chang J, Xiao Y. Multidirectional effects of Sr-, Mg-, and Si-containing bioceramic coatings with high bonding strength on inflammation, osteoclastogenesis, and osteogenesis. ACS Appl Mater Interfaces. 2014;6(6):4264–76.
2. Kokubo T. Surface chemistry of bioactive glass-ceramics. J Non Cryst Solids. 1990;120:138–51.
3. Sun J, Li J, Liu X, Wei L, Wang G, Meng F. Proliferation and gene expression of osteoblasts cultured in DMEM containing the ionic products of dicalcium silicate coating. Biomed Pharmacother. 2009;63(9):650–7.

4. Liu XY, Xie YT, Ding CX, Chu PK. Early apatite deposition and osteoblasts growth on plasma sprayed dicalcium silicate coating. J Biomed Mater Res. 2005;74A:356–65.
5. Gandolfi MG, Ciapetti G, Perut F, Taddei P, Modena E, Rossi PL, Prati C. Biomimetic calcium-silicate cements aged in simulated body solutions. Osteoblast response and analyses of apatite coating. J Appl Biomater Biomech. 2009;7(3):160–70.
6. Gandolfi MG, Ciapetti G, Taddei P, Perut F, Tinti A, Cardoso MV, Van Meerbeek B, Prati C. Apatite formation on bioactive calcium-silicate cements for dentistry affects surface topography and human marrow stromal cells proliferation. Dent Mater. 2010;26(10):974–92.
7. Wu BC, Wei CK, Hsueh NS, Ding SJ. Comparative cell attachment, cytotoxicity and antibacterial activity of radiopaque dicalcium silicate cement and white-coloured mineral trioxide aggregate. Int Endod J. 2015;48(3):268–76.
8. Chiang TY, Ding SJ. Comparative physicochemical and biocompatible properties of radiopaque dicalcium silicate cement and mineral trioxide aggregate. Journal of Endod. 2010;36(10):1683–7.
9. Gou Z, Chang J, Zhai W, Wang J. Study on the self-setting property and the in vitro bioactivity of beta-Ca2SiO4. J Biomed Mater Res B. 2005;73(2):244–51.
10. Liu X, Tao S, Ding C. Bioactivity of plasma sprayed dicalcium silicate coatings. Biomaterials. 2002;23(3):963–8.
11. Hirakawa K, Jacobs JJ, Urban R, Saito T. Mechanisms of failure of total hip replacements: lessons learned from retrieval studies. Clin Orthop Relat Res. 2004;420:10–7.
12. Pazár B, Ea HK, Narayan S, Kolly L, Bagnoud N, Chobaz V, Roger T, Lioté F, So A, Busso N. Basic calcium phosphate crystals induce monocyte/macrophage IL-1β secretion through the NLRP3 inflammasome in vitro. J Immunol. 2011;186(4):2495–502.
13. Ion R, Stoian AB, Dumitriu C, Grigorescu S, Mazare A, Cimpean A, Demetrescu I, Schmuki P.Nanochannels formed on TiZr alloy improve biological response. Acta biomateriala. 2015, 16, S1742-7061(15)00282-2.
14. Velard F, Laurent-Maquin D, Braux J, Guillaume C, Bouthors S, Jallot E, Nedelec JM, Belaaouaj A, Laquerriere P. The effect of zinc on hydroxyapatite-mediated activation of human polymorphonuclear neutrophils and bone implant-associated acute inflammation. Biomaterials. 2010;31(8):2001–9.
15. Kaufman AM, Alabre CI, Rubash HE, Shanbhag AS. Human macrophage response to UHMWPE, TiAlV, CoCr, and alumina particles: analysis of multiple cytokines using protein arrays. J Biomed Mater Res A. 2008;84(2):464–74.
16. Jones JR, Hench LL. Effect of surfactant concentration and composition on the structure and properties of sol–gel-derived bioactive glass foam scaffolds for tissue engineering. J Biomed Mater Res B. 2004;68(1):36–44.
17. Laquerriere P, Grandjean-Laquerriere A, Jallot E, Balossier G, Frayssinet P, Guenounou M. Importance of hydroxyapatite particles characteristics on cytokines production by human monocytes in vitro. Biomaterials. 2003;24(16):2739–47.
18. Buache E, Velard F, Bauden E, Guillaume C, Jallot E, Nedelec JM, Laurent-Maquin D, Laquerriere P. Effect of strontium-substituted biphasic calcium phosphate on inflammatory mediators production by human monocytes. Acta Biomater. 2012;8(8):3113–9.
19. Laquerriere P, Grandjean-Laquerriere A, Addadi-Rebbah S, Jallot E, Lauernt-Maquin D, Frayssinet P. MMP-2, MMP-9 and their inhibitors TIMP-2 and TIMP-1 production by human monocytes in vitro in presence of differents hydroxyapatite: importance of particle physical characteristics. Biomaterials. 2004;25(13):2515–24.
20. Liangjiao C, Ping Z, Ruoyu L, Yanli Z, Ting S, Yanjun L, Longquan S. Potential proinflammatory and osteogenic effects of dicalcium silicate particles in vitro. J Mech Behav Biomed Mater. 2014;44:10–22.
21. Varanasi VG, Saiz E, Loomer PM, Ancheta B, Uritani N, Ho SP, Tomsia AP, Marshall SJ, Marshall GW. Enhanced osteocalcin expression by osteoblast-like cells (MC3T3-E1) exposed to bioactive coating glass (SiO_2–CaO–P_2O_5–MgO–K_2O–Na_2O system) ions. Acta Biomater. 2009;5(9):3536–47.
22. Newman SD, Lotfibakhshaiesh N, O'Donnell M, Walboomers XF, Horwood N, Jansen JA, Amis AA, Cobb JP, Stevens MM. Enhanced osseous implant fixation with strontium-substituted bioactive glass coating. Tissue Eng A. 2014;20(13–14):1850–7.
23. Eberhard J, Reimers N, Dommisch H, Hacker J, Freitag S, Acil Y, Albers HK, Jepsen S. The effect of the topical administration of bioactive glass on inflammatory markers of human experimental gingivitis. Biomaterials. 2005;26(13):1545–51.
24. Day RM, Boccaccini AR. Effect of particulate bioactive glasses on human macrophages and monocytes in vitro. J Biomed Mater Res A. 2005;73(1):73–9.
25. Bosetti M, Hench L, Cannas M. Interaction of bioactive glasses with peritoneal macrophages and monocytes in vitro. J Biomed Mater Res. 2002;60(1):79–85.
26. Li J, Wei L, Sun J, Guan G. Effect of ionic products of dicalcium silicate coating on osteoblast differentiation and collagen production via TGF-β1 pathway. J Biomater Appl. 2013;7(5):595–604.
27. Cacciotti I, Lombardi M, Bianco A, Ravaglioli A, Montanaro L. Sol-gel derived 45S5 bioglass: synthesis, microstructural evolution and thermal behaviour. J Mater Sci Mater Med. 2012;23(8):1849–66.
28. Velasquez P, Luklinska ZB, Meseguer-Olmo L, de Val Mate-Sanchez JE, Delgado-Ruiz RA, Calvo-Guirado JL, Ramirez-Fernandez MP, de Aza PN. αTCP ceramic doped with dicalcium silicate for bone regeneration applications prepared by powder metallurgy method: in vitro and in vivo studies. J Biomed Mater Res A. 2013;101(7):1943–54.
29. Meseguer-Olmo L, Aznar-Cervantes S, Mazón P, De Aza PN. "In vitro" behavior of adult mesenchymal stem cells of human bone marrow origin seeded on a novel bioactive ceramics in the Ca_2SiO_4-$Ca_3(PO_4)_2$ system. J Mater Sci Mater Med. 2012;23(12):3003–14.
30. Nelson GM, Nychka JA, McDonald AG. Structure, phases, and mechanical response of Ti-alloy bioactive glass composite coatings. Mater Sci Eng C Mater Biol Appl. 2014;36:261–76.
31. Khor KA, Gu YW, Pan D, Cheang P. Microstructure and mechanical properties of plasma sprayed HA/YSZ/Ti–6Al–4V composite coatings. Biomaterials. 2004;25(18):4009–17.
32. Kitsugi T, Nakamura T, Oka M, Senaha Y, Goto T, Shibuya T. Bone-bonding behavior of plasma-sprayed coatings of BioglassR, AW-glass ceramic, and tricalcium phosphate on titanium alloy. J Biomed Mater Res. 1996;30(2):261–9.
33. Scislowska-Czarnecka A, Menaszek E, Szaraniec B, Kolaczkowska E. Ceramic modifications of porous titanium: effects on macrophage activation. Tissue Cell. 2012;44(6):391–400.
34. Curran JM, Gallagher JA, Hunt JA. The inflammatory potential of biphasic calcium phosphate granules in osteoblast/macrophage coculture. Biomaterials. 2005;26(26):5313–20.
35. de Aza PN, Luklinska ZB, de Val Mate-Sanchez JE, Calvo-Guirado JL. Biodegradation process of α-tricalcium phosphate and α-tricalcium phosphate solid solution bioceramics in vivo: a comparative study. Microsc Microanal. 2013;19(5):1350–7.
36. Jakobsen SS, Larsen A, Stoltenberg M, Bruun JM, Soballe K. Hydroxyapatite coatings did not increase TGF-beta and BMP-2 secretion in murine J774A.1 macrophages, but induced a pro-inflammatory cytokine response. J Biomater Sci Polym Ed. 2009;20(4):455–65.
37. Ding H, Zhu Z, Tang T, Yu D, Yu B, Dai K. Comparison of the cytotoxic and inflammatory responses of titanium particles with different methods for endotoxin removal in RAW264.7 macrophages. J Mater Sci Mater Med. 2012;23(4):1055–62.

38. Li HW, Sun JY. Effects of dicalcium silicate coating ionic dissolution products on human mesenchymal stem-cell proliferation and osteogenic differentiation. J Int Med Res. 2011;39(1):112–28.
39. Sun J, Wei L, Liu X, Li J, Li B, Wang G, Meng F. Influences of ionic dissolution products of dicalcium silicate coating on osteoblastic proliferation, differentiation and gene expression. Acta Biomater. 2009;5(4):1284–93.
40. Lee TM, Tsai RS, Chang E, Yang CY, Yang MR. Biological responses of neonatal rat calvarial osteoblasts on plasma-sprayed HA/ZrO2 composite coating. J Mater Sci Mater Med. 2002;13(3):281–7.
41. van Oirschot BA, Alghamdi HS, Närhi TO, Anil S, Al Farraj Aldosari A, van den Beucken JJ, Jansen JA. In vivo evaluation of bioactive glass-based coatings on dental implants in a dog implantation model. Clin Oral Implants Res. 2014;25(1):21–8.
42. Li J, Wei L, Sun J, Guan G. Effect of ionic products of dicalcium silicate coating on osteoblast differentiation and collagen production via TGF-β1 pathway. J Biomater Appl. 2013;27(5):595–604.
43. Liu X, Ding C, Chu PK. Mechanism of apatite formation on wollastonite coatings in simulated body fluids. Biomaterials. 2004;25(10):1755–61.
44. De Aza PN, García-Bernal D, Cragnolini F, Velasquez P, Meseguer-Olmo L. The effects of Ca2SiO4-Ca3(PO4)2 ceramics on adult human mesenchymal stem cell viability, adhesion, proliferation, differentiation and function. Mater Sci Eng C Mater Biol Appl. 2013;33(7):4009–20.
45. Li J, Wei L, Sun J, Guan G. Effect of ionic products of dicalcium silicate coating on osteoblast differentiation and collagen production via TGF-β1 pathway. J Biomater Appl. 2013;27(5):595–604.
46. Varanasi VG, Owyoung JB, Saiz E, Marshall SJ, Marshall GW, Loomer PM. The ionic products of bioactive glass particle dissolution enhance periodontal ligament fibroblast osteocalcin expression and enhance early mineralized tissue development. J Biomed Mater Res A. 2011;98(2):177–84.
47. Silva JM, Zupancic E, Vandermeulen G, Oliveira VG, Salgado A, Videira M, Gaspar M, Graca L, Préat V, Florindo HF. In vivo delivery of peptides and Toll-like receptor ligands by mannose-functionalized polymeric nanoparticles induces prophylactic and therapeutic anti-tumor immune responses in a melanoma model. J Control Release. 2015;198(28):91–103.
48. Mano SS, Kanehira K, Taniguchi A. Comparison of cellular uptake and inflammatory response via toll-like receptor 4 to lipopolysaccharide and titanium dioxide nanoparticles. Int J Mol Sci. 2013;14(7):13154–70.
49. Pearl JI, Ma T, Irani AR, Huang Z, Robinson WH, Smith RL, Goodman SB. Role of the Toll-like receptor pathway in the recognition of orthopedic implant wear-debris particles. Biomaterials. 2011;32(24):5535–42.
50. Landgraeber S, Jäger M, Jacobs JJ, Hallab NJ. The pathology of orthopedic implant failure is mediated by innate immune system cytokines. Mediators Inflamm. 2014;2014:185150.
51. Refai AK, Textor M, Brunette DM, Waterfield JD. Effect of titanium surface topography on macrophage activation and secretion of proinflammatory cytokines and chemokines. J Biomed Mater Res A. 2004;70(2):194–205.
52. Kai Soo Tana. Li Qiana, Roy Rosadob, Patrick M. Flooda, c, d, Lyndon F. Cooper. The role of titanium surface topography on J774A.1 macrophage inflammatory cytokines and nitric oxide production. Biomaterials. 2006;27(30):5170–7.
53. Hamlet Stephen, Ivanovski Saso. Inflammatory cytokine response to titanium chemical composition and nanoscale calcium phosphate surface modification. Acta Biomater. 2011;7(5):2345–53.
54. Moura CC, Machado JR, Silva MV, Rodrigues DB, Zanetta-Barbosa D, Jimbo R, Tovar N, Coelho PG. Evaluation of human polymorphonuclear behavior on textured titanium and calcium-phosphate coated surfaces. Biomed Mater. 2013;8(3):035010.
55. Scislowska-Czarnecka A, Menaszek E, Szaraniec B, Kolaczkowska E. Ceramic modifications of porous titanium: effects on macrophage activation. Tissue Cell. 2012;44(6):391–400.